Stabilization of 3d-transition metal hydrido complexes in SrH2Mg2[Co(I)H5], BaH2Mg5[Co(-I)H4]2 and RbH2Mg5[Co(-I)H4 Ni(0)H4] with a novel "back donation" mechanism

Journal:	*Inorganic Chemistry*
Manuscript ID:	Draft
Manuscript Type:	Article
Date Submitted by the Author:	n/a
Complete List of Authors:	Fahlquist, Henrik; Stockholm University, Materials and Environmental Chemistry Moser, David; Institute for Renewable Energy, Noréus, Dag; Stockholm University, Materials and Environmental Chemistry Refson, Keith; STFC Rutherford Appleton Laboratory, CSE Parker, Stewart; Rutherford Appleton Laboratory, ISIS Facility

Stabilization of 3d-transition metal hydrido complexes in $SrH_2Mg_2[Co(I)H_5]$, $BaH_2Mg_5[Co(-I)H_4]_2$ and $RbH_2Mg_5[Co(-I)H_4\ Ni(0)H_4]$ with a novel "back donation" mechanism

Henrik Fahlquist,[1] David Moser,[1$] Dag Noréus,[1] Keith Refson[2] and Stewart F. Parker[3]

[1]Department of Materials and Environmental Chemistry, Arrhenius Laboratory, Stockholm University, S-106 91 Stockholm, Sweden

[2]Computational Science and Engineering Department, STFC Rutherford Appleton Laboratory, Chilton, Didcot, OX11 0QX, UK

[3]ISIS Facility, STFC Rutherford Appleton Laboratory, Chilton, Didcot, Oxon OX11 0QX, UK.

$ Current address: Institute for Renewable Energy, EURAC, 39100 Bolzano, Italy

Abstract

A combined study using neutron diffraction, inelastic scattering and first principle calculations describe cobalt with a very low formal oxidation state of (-I) in a slightly distorted tetrahedral $Co(-I)H_4$-complex in $BaH_2Mg_5[Co(-I)H_4]_2$ and in the structurally related $RbH_2Mg_5[Co(-I)H_4\ Ni(0)H_4]$. This indicates that the electron "back donating" effect via the polarisable hydride ions to the counter ions in the solid state hydrides, can be compared to more conventional "back bonding" able to reduce the oxidation state down to -I. The hydrides were synthesised by hot sintering of transition metal powders with corresponding binary alkali- and alkaline earth hydrides. In the similarly synthesized $SrH_2Mg_2[Co(I)H_5]$, cobalt is formally +I-valent, showing a high sensitivity to differences in the counter ion framework, which can also influence electrical properties.

Introduction

If electropositive alkali and alkaline earth metals are reacted under hydrogen with transition metals (TM) to the right of group V, the TM is likely to form TM-hydrido complexes with the valence electrons from the electropositive metals. The bonding in the complexes has mainly an sd-electron character. This makes 4d- and 5d TM-hydrido complexes strong, since the soft 4d- and 5d orbitals are better suited to the very polarisable and soft hydride ions. The stability of the corresponding ternary hydrides becomes too high for practical applications, in addition these metals are prohibitively expensive. More interesting is the 3d TM-hydrido complexes. The 3d-electrons are not so well suited to bonding with hydrogen and to stabilize the complexes, help is needed from a strongly polarizing counter ion i. e. Mg^{2+}.[1,2] A much

investigated example is the Mg_2NiH_4 system. Several hundred papers have been written to date and the system still attracts interest for possible hydrogen storage. In Mg_2NiH_4 nickel forms an 18 electrons, tetrahedral formally zero-valent $[Ni(0)H_4]$-complex, with the help of the valence electrons from magnesium. However, the strongly polarizing Mg^{2+} has another significant influence on the electronic structure of this type of hydrides. Without Mg in the counterion lattice, the electronic structures of the complexes are very "molecular like" and the bands can be easily identified with their molecular orbital counter parts, as they are essentially flat in the electronic density of states (eDOS).[2] With the strongly polarizing Mg^{2+} ion the bands become dispersed and overlapping. This implies unusual and interesting bonding properties making Mg_2NiH_4 interesting also from a fundamental solid state physics perspective. The central nickel atom is in an electron rich formal zero-valent d^{10} oxidation state. Such low oxidation states usually require strong electron accepting ligands, which can transfer some electron density from the central nickel atom by "back donation" to the ligand orbitals. In the solid state polarizing Mg^{2+} ions can relieve some of this electron density via the very polarisable hydride ion. This reduces the molecular character of the $[Ni(0)H_4]$-complex and makes the ternary hydride more stable, but also more metal like. We have recently shown how subtle changes in the counter ion lattice have a profound influence on the electron conductivity, switching it from a conductor to an insulator with the help of a stacking fault in the lattice, that changes the band gap.[3] The stabilizing influence of the Mg^{2+} ions is, however, strong and the stability of Mg_2NiH_4 is still too high for any practical application to have evolved. In an effort to reduce the stability, trials to partially substitute the Mg^{2+} ions with less polarizing counter ions has been attempted.[4] However, few hydrides based on 3d-TM complexes have been synthesized without having magnesium as a counter ion limiting the number of such hydrides found to date.

The purpose of the present paper was to investigate how hydrogen complexes with the neighbouring transition metal cobalt reacted to substitutions of Mg^{2+} ions with softer and less polarizing counter ions. A low formal oxidation state in a $[Co(-I)H_4]$-complex could be stabilized in $BaH_2Mg_5[Co(-I)H_4]_2$ with the help of more electropositive and less polarizing Ba^{2+} ions. By substituting the Ba^{2+} ions with Rb^+ ions, the structure can essentially be retained in $RbH_2Mg_5[Co(-I)H_4\ Ni(0)H_4]$ if a corresponding number of $[Co(-I)H_4]$-complexes are substituted by $[Ni(0)H_4]$ –complexes. This indicates the importance of the electron count for forming these hydrides. In $SrH_2Mg_2[Co(I)H_5]$ the higher formal oxidation state of +I for cobalt is maintained, when Mg^{2+} is partly substituted by with Sr^{2+}, which is not so soft as Ba^{2+} and Rb^+.

The electron dense complexes are hydrogen rich with interesting electron conductivity properties related to how the lattice helps to relieve the high electron density in the complexes. We believe that they are interesting enough to be studied in more detail and not only for their high hydrogen contents.

Experimental

Synthesis

All starting materials and samples were handled inside a continuously purified argon filled glove box. Heat treatment was done by placing pressed pellets of ground powders in aluminium oxide tubes heated in stainless steel reactors placed in a tube furnace. The temperature was monitored by contacting a thermocouple in a sealed stainless steel capillary to the sample.

BaH_2 was made by reacting barium pieces from Sigma Aldrich to 573 K in 20 bar H_2 atmosphere overnight yielding white brittle pieces of BaH_2. Mg_2CoH_5 was made by heat treatment of pelletized MgH_2 and Co metal powders in the molar ratio 2:1 in 70 bar of H_2 at 773 K for 18 hours, resulting in black Mg_2CoH_5.

Mg_2NiH_4 was produced by reacting pulverized Mg_2Ni alloy in a 40 bar H_2 atmosphere at 623 K. The hydride was cycled five times by releasing and restoring the hydrogen pressure over a period of 8 hours to obtain a fully hydrided brown sample.

$BaH_2Mg_5[CoH_4]_2$ was made by mixing BaH_2, Mg_2CoH_5 and MgH_2 in the molar ratio 1:2:1 using a pestle and mortar. The powder mixture was pelletized and heat treated in 70 bar H_2 at 833 K for 18 hours. The resulting product was a single phase black powder.

$RbH_2Mg_5[CoH_4][NiH_4]$ was made by mixing Rb, Mg_2CoH_5, Mg_2NiH_4 and MgH_2 in the molar ratio 1:1:1:1 using a pestle and mortar. The powder was pelletized and heat treated in 70 bar H_2 at 773 K for 18 hours. The resulting product was a single phase dark purple powder.

$Ba_{0.5}Rb_{0.5}H_2Mg_5[CoH_4]_{1.5}[NiH_4]_{0.5}$ was prepared in the same way as $RbH_2Mg_5[CoH_4][NiH_4]$ to yield a single phase black powder.

$SrH_2Mg_2[CoH_5]$ was made by mixing powders of SrH_2 and MgH_2 and Co powder in the molar ratio 1:2:1. The powder mixture was ground to a fine powder using a pestle and mortar and pelletized and heat treated in 70 bar H_2 at 815 K for 18 hours. The resulting product was an almost single phase black powder. To establish the optimum reaction conditions and reactant ratios given above, a rather time consuming trial and error procedure was required, where the reaction conditions were varied and after each run a small sample was removed for XRD

analysis. To produce samples for neutron diffraction, deuterated analogues were produced using the corresponding deuterides and D_2 gas.

Structural investigations

X-ray diffraction patterns were obtained on a Panalytical X'pert pro powder diffractometer equipped with a germanium [111] monochromator (λ=1.540598 Å). Indexing of the unit cells were performed using the TREOR[5] feature in the software Panalytical Highscore Plus. From systematic extinctions, the unit cell of $BaH_2Mg_5[CoH_4]_2$ was assigned to the space group *Immm* (71) by choosing the highest symmetry body centred space group. The unit cell was then refined in Panalytical Highscore Plus by least squares with resulting refined lattice parameters a= 7.392(2) Å, b= 11.602(4) Å, c= 4.6265(9) Å. For $RbH_2Mg_5[CoH_4][NiH_4]$, the lattice parameters were refined to a=7.345(6) Å, b=11.877(8) Å and c=4.703(3) Å and the structure was also initially assigned to the space group *Immm* (71). The initial structures were solved in FOX[6] and the metal atom parameters were refined in Fullprof2000.

The least squares refinement of $RbH_2Mg_5[CoH_4][NiH_4]$ indicated a lower symmetry and the space group had to be changed to *Imm2* (44), the final agreement factors were R_{wp}=0.0312 and R_p=0.0207 for the X-ray structure refinement.

The diffraction pattern for $SrH_2Mg_2[CoH_5]$ was indexed with a monoclinic cell with lattice parameters a=7.818(2) Å, b=4.462(1) Å, c=6.640(2) Å and β=91.27(2)° and the space group *C12/m1* (12) was assigned from extinction criteria and choosing the highest symmetry.

To elucidate the hydrogen positions, neutron powder patterns were obtained from the corresponding deuterides at the time-of-flight instrument GEM at ISIS using a sealed cylindrical ø=5 mm vanadium sample holder.

The initial deuterium positions were obtained using simulated annealing in FOX[6] keeping the metal positions fixed. The full structure refinement was performed by least squares refinement in GSAS[7].

The unit cell for $BaH_2Mg_5[CoD_4]_2$ was refined to a=7.39919 Å, b=11.570691 Å and c=4.622355 Å, slightly smaller than the hydride indicating anharmonic hydrogen vibrations that are commonly observed in these types of hydrides. R_{wp}=0.0223 and R_p=0.0165 for the full structure refinement. The structure with well separated and aligned but slightly distorted tetrahedral CoD_4 complexes is shown in **Figure 1**. The complexes nearest neighbours are all Mg^{2+} ions whereas the Ba^{2+} ions are found in "BaH_2" related layers separating "$Mg_5[CoD_4]_2$"

layers. Refined atom positions are listed in **Table 1.** Distances and angles can be found in **Table 2.**

The structure of $RbMg_5[CoD_4][NiD_4]$ was found to be closely related to that of $BaH_2Mg_5[CoD_4]_2$. Due to problems with a disordered arrangement of the Co- and Ni-complexes and a lower symmetry, the detailed structure could not be elucidated at this point. The metal atom positions could, however, be refined and the main difference to the metal atom structure in $BaH_2Mg_5[CoD_4]_2$ is a slight shift of one of the magnesium positions as illustrated in **Figure 2**. **Table 3a** lists the metal atom positions for $RbMg_5[CoD_4][NiD_4]$. **Table 3b** shows that partial substitutions of alkali earth/alkali- metal and transition metals could be made leading to a continuous transition between the structures, if the 18-electron count is kept for the complexes.

The magnesium atom shift can not be accommodated in the centrosymmetric space group *Immm* (71), however, and the use of the non-centrosymmetric space group *Imm2* (44) unfortunately increases the number of structural parameters to be refined, leading to instability problems in the refinements. Constraining the parameters can improve the stability but the result would be biased. The general picture is, however, that the tetragonal complexes are kept but their orientations are more disordered than the uniform alignment in the $BaH_2Mg_5[CoD_4]_2$ structure. Below it will also be shown that this leads to a smearing out of the vibrational frequencies in $RbMg_5[CoH_4][NiH_4]$ compared to $BaH_2Mg_5[CoH_4]_2$ although both exhibit similar general features.

The unit cell for $SrD_2Mg_2[CoD_5]$ was refined to a=7.8140(3) Å, b=4.4593(2) Å, c=6.6347(2) Å and β=91.237(3)°. The space group had to be changed to *P12$_1$/n1* (11) for the deuteride since the deuterium structure breaks the C-symmetry. The agreement factors became R_{wp}=0.0378 and R_p=0.0297, for the full structure refinement.

The refined atom positions are listed in **Table 4** and distances and angles in **Table 5.** The contents of the unit cell are illustrated in **Figure 3.** A summary of the lattice parameters and the agreement factors for all the structures can be found in **Table 6.** All hydrides contain hydrogen both in interstitial sites and bound in complexes.

Calculations - CASTEP

Periodic DFT calculations of the crystalline structures were carried out using the plane-wave pseudopotential method implemented in the CASTEP code.[8,9] Exchange and correlation were approximated in the local density approximation (LDA) using the CA-PZ[10,11]

parameterization. Optimized norm-conserving pseudopotentials[12] were used with a plane-wave cut-off of 990 eV. The equilibrium structure, an essential prerequisite for lattice dynamics calculations was obtained by BFGS geometry optimization after which the residual forces were converged to zero within 0.009 eV/Å. Phonon frequencies were obtained by diagonalisation of dynamical matrices computed using density-functional perturbation theory[9] (DFPT). An analysis of the resulting eigenvectors was used to map the computed modes to the corresponding irreducible representations of the point group and assign IUPAC symmetry labels. In addition to the direct evaluation of frequencies and intensities at zero wavevector, phonon dispersion was calculated along high symmetry directions throughout the Brillouin zone. For this purpose, dynamical matrices were computed on a regular grid of wavevectors throughout the Brillouin zone and Fourier interpolation was used to extend the computed grid to the desired fine set of points along the high-symmetry paths.[12]

The program ACLIMAX[13] was used to produce the INS spectrum from the *ab initio* results.

Inelastic neutron scattering

INS spectra were obtained with the spectrometers TOSCA[14] and MAPS[15] at ISIS.[16] The instruments are highly complementary: TOSCA has excellent resolution at <1400 cm^{-1} while MAPS provides access to higher energy transfer. Incident energies (E_i) of 4033 and 2420 cm^{-1} were used. For the INS measurements the samples were loaded into indium wire sealed aluminium cans in a glovebox. The spectra were recorded at <20 K for 7-10 hours. INS spectroscopy[14] has several advantages that make it valuable for the study of complex metal hydrides.[16] The spectral intensity, $S(Q,\omega)$, depends on the product of the incoherent cross section and the amplitude of vibration of the atoms in the mode. Hydrogen, ^1H, is both the lightest element (hence has the largest amplitude of vibration) and has the largest cross section, thus motions that involve hydrogen will dominate the spectrum. Further, since the scattering is purely dynamic, the symmetry requirements resulting from the interaction of light with electrons that give rise to selection rules for infrared and Raman spectroscopies are absent and all modes are allowed.

Results and Discussion.

In Mg_2CoH_5 a $Co(I)H_5$ complex with a square planar pyramidal structure is surrounded by magnesium counter ions and the formal oxidation state is +1. By substituting some of the magnesium with the more electropositive and less polarizing barium the formal oxidation state was reduced to a surprisingly low -1 in $BaH_2Mg_5(Co(-I)H_4)_2$. In our DFT calculations

this increased the band gap from 0.3 eV to close to 1 eV. The barium could be further substituted by rubidium but in order to keep the electron count correct for the 18 electron complexes, cobalt has also to be partly substituted by nickel. This led to $RbH_2Mg_5[Co(-I)H_4][Ni(0)H_4]$ with a structure closely related to that of $BaH_2Mg_5[Co(-I)H_4]_2$. It is further possible to continuously move between these limiting compositions. (Table 3a and b) Due to the disorder in the structure no DFT calculation was performed. But the colour change from black to dark red with increasing Rb content indicates an increasing band gap.

In $SrH_2Mg_2[CoH_5]$ the DFT calculation shows a decreased band gap of 0.07 eV. This was also corroborated by a simple measurement of the electric resistivity using a standard Ohmmeter. Pressed tablets of $SrH_2Mg_2[CoH_5]$ are conducting at room temperature. However, if the temperature is reduced by cooling the tablet with liquid nitrogen, the measurable conductivity disappears but is restored when the temperature is increased.

Figure 4 compares the INS spectra of the three compounds recorded on TOSCA. It can be seen that while $SrH_2Mg_2[Co(I)H_5]$ and $BaH_2Mg_{10}[Co(-I)H_4]_2$ give well-resolved spectra while the mixed complex $RbH_2Mg_{10}[Co(-I)H_4\ Ni(0)H_4]$ gives very broad bands with little hint of any structure, consistent with the disorder present.

Figure 5 shows the INS spectra of $BaH_2Mg_{10}[Co(-I)H_4]_2$ recorded on MAPS. The lower part is obtained by summing over the momentum transfer with two different incident energies. With $E_i = 2420\ cm^{-1}$ the Co–H stretching modes at 1678 and 1788 cm^{-1} are easily observed, while with $E_i = 4033\ cm^{-1}$ two weak bands at 3287 and 3517 cm^{-1} with a shoulder at 3466 cm^{-1} are apparent. These are assigned as the first overtone of each of the stretching modes and the combination mode and clearly there is significant anharmonicity present since the predicted overtones would be at 3356 and 3576 cm^{-1}. This is consistent with the difference in unit cell parameters of the hydrides and deuterides.

The spectra can be summarised as: M–H stretching modes 1600 - 1900 cm^{-1}, H–M–H bending modes and H^- translations 700 – 1200 cm^{-1}, complex ion librational modes 350- 700 cm^{-1} and heavy atom translation modes (acoustic and optic) 0 – 350 cm^{-1}. To go beyond this simple description, additional information is required which can be obtained from the CASTEP *ab initio* calculations. These were initially carried out with generalized gradient approximation (GGA) and the PBE functional.[17] While the geometry optimisation was straightforward, we invariably found that the calculation of the vibrational transition energies resulted in imaginary modes. Varying the convergence criteria or choice of pseudopotentials did not change this situation. It was eventually found that all real modes could be obtained using

LDA with the CA-PZ[10,11] functional and all the calculations reported here were carried out using this approach.

Tables 1-4 and **4-5** include the calculated structural parameters for $BaH_2Mg_5[Co(\text{-}I)H_4]_2$ and $SrH_2Mg_2[Co(I)H_5]$ and **Tables 7-8** those for $Mg_2[Co(I)H_5]$. It can be seen that in all cases the calculated values are very close to those observed experimentally: bond distances are all within 0.1 Å and bond angles are generally within a few degrees. For all the complexes there is a tendency that the variation in bondlengths is less marked in the calculations than is observed experimentally, although the trends are always correct, *e.g.* for $SrH_2Mg_2[Co(I)H_5]$ the observed Co–H distances are 1.65 and 1.52 Å, while the calculated distances are 1.603 and 1.566 Å. These distances are also slightly longer than are found (experimentally and computationally) in $Mg_2[Co(I)H_5]$.

For $BaH_2Mg_5[Co(\text{-}I)H_4]_2$ and $SrH_2Mg_2[Co(I)H_5]$ the CASTEP calculations show that there is significant dispersion in the modes as shown by the dispersion curves, **Figures 6** and **7** and comparison of the observed and calculated spectra, **Figures 8** and **9**. It can be seen that the spectra generated from the calculation across the entire Brillouin zone are in much better agreement with the experimental spectra than those from a calculation at just the Γ-point. This is a reflection that INS spectra are allowed at all momentum transfer values, not just at Q ~0 as for infrared and Raman spectra. The long range interactions evidenced by the spectra emphasise the need for fully periodic calculations in these systems. The interaction is most likely to be the result of the Coulombic interactions between the ions as was found for $Ba[ReH_9]$.[18] Animations of the modes enables assignments to be made and these are given in **Tables 9** and **10** for the Γ-point modes of $BaH_2Mg_5[Co(\text{-}I)H_4]_2$ and $SrH_2Mg_2[Co(I)H_5]$ respectively.

Since the INS spectrum is purely dynamic, we can investigate the contributions of the individual species separately. By setting the cross-section of all the atoms to zero, except for the atoms of interest, only the modes involving motion of those atoms will contribute to the calculated INS spectrum. **Figures 10** and **11** show the results and support the assignments given in **Tables 9** and **10**. Thus for $BaH_2Mg_5[Co(\text{-}I)H_4]_2$ the $[Co(\text{-}I)H_4]^{5-}$ ion has translational modes below 200 cm^{-1}, librational modes around 400 cm^{-1}, H–Co–H bending modes at 500 – 700 cm^{-1} and Co–H stretching modes at 1650 – 1850 cm^{-1}. If the cobalt atom is considered in isolation then the pattern looks very similar except that there is very little intensity in the librational region as expected since, to a first approximation, the centre of mass is invariant during a libration. The interstitial hydrides exhibit relatively pure modes at 600 – 750 cm^{-1} and 900 – 1000 cm^{-1} and account for most of the intensity in this region. The translational

modes of the magnesium ions are all at < 450 cm^{-1} with those of the barium ion largely below 200 cm^{-1}. As might be expected, below 450 cm^{-1} there is significant mixing of modes and there are no pure modes. A similar pattern is found for $SrH_2Mg_2[Co(I)H_5]$ with the Sr^{2+}, Mg^{2+} and H^- modes at energies close to those found in the barium containing compound. The librational and deformational modes of the complex ion occur at somewhat higher energies than those found in the barium containing compound: librations at 500 – 700 cm^{-1}, H–Co–H bending modes at 700 – 1000 cm^{-1} while the Co–H stretching modes at 1600 – 1850 cm^{-1} are at comparable energies.

Evidence from both INS spectra and electronic structure calculations points to a close similarity in the electronic structures of the cobalt complexes in all three compounds. **Figure 12 a,b** shows a comparison of the experimental INS spectrum of $Mg_2[Co(I)H_5]$[19] and that of the $[Co(I)H_5]^{4-}$ in $SrH_2Mg_2[Co(I)H_5]$ generated by considering only the hydrides bonded to the cobalt. It can be seen that the degree of similarity is remarkable; the only significant difference is that the librational modes in the strontium complex are 10 – 20% higher in energy than in the parent compound. The similarity in the transition energies of the stretching modes would indicate that the bonds are also of similar strength, although the degeneracies are lifted, **Figure 12 c**, by virtue of the site symmetry, C_s *vs.* C_{4v}. CASTEP calculations of the Born effective charges of the $[CoH_5]$ units yield almost identical values with diagonal components (-4.0,-4.0, -3.9) [Mg] and (-4.1,-4.0,-3.5)[Sr] in these two cases, also indicating very similar electronic environments. By contrast with static population analysis the Born charges characterize the electron dynamics and are usually close to formal ionic charges. The effective charge on the corresponding cations is +2.2 ([Mg] and +2.3[Sr]. Surprisingly, the barium complex that contains $[Co(-I)H_4]^{5-}$ ions has similar stretching energies, despite the cobalt being in a lower oxidation state. In that case the Born effective charges are slightly more negative at (-4.5,-4.8, -4.7) on $[Co(-I)H_4]$, close to the formal -5, with +2.8 on Ba. The electropositive counterions push different degrees of electrons on to the complexes, but the polarizing Mg^{2+} ions can help to redistribute the electrons *via* the hydrogen atoms. A static Hirshfeld population analysis from the DFT calculations supports these trends, despite yielding results much smaller than formal ionic charge states. Ba and Sr get a similar Hirshfeld charge of 0.29 e in both hydrides. Co(-I) and Co(+I) get -0.33 and -0.29 e, respectively. The interstitial hydrogen atoms are more ionic with a charge of -0.15 e in both compounds compared to the hydrogen in the complexes, which have a charge of -0.07 and -0.09 in the Co(+I) and Co(-I) complex, respectively. Finally the magnesium atoms in the Co(-I) hydride is less positive with a Hirshfeld charge of 0.29 e compared to 0.32 e for the

Co(+I) hydride. The delicate balance of these electron redistributions seems to be intricately dependent on the size and electropositivity of the counter ions. It is interesting, however, that the formal oxidation state has greater implication for more subtle effects such as the band gap. Both $Mg_2Co(I)H_5$ and $SrH_2Mg_2[Co(I)H_5]$ have very small bandgaps and are more metallic than $BaH_2Mg_5[Co(-I)H_4]_2$ and also $RbH_2Mg_{10}[Co(-I)H_4\ Ni(0)H_4]$ both with bandgaps above 1 eV.

Acknowledgements

The Rutherford Appleton Laboratory is thanked for access to neutron beam facilities. Computing resources (time on the SCARF computer used to perform the CASTEP calculations) was provided by STFC's e-Science facility. This work has been financially supported the Swedish Energy Agency.

Tables

Table 1. Lattice parameters, atom positions and temperature parameters of $BaD_2Mg_5[Co(-I)D_4]_2$ in space group *Immm* (62), statistical uncertainties (SU) in parentheses. Experimental values are in normal type, those calculated by CASTEP are in italics.

Atom	Wyckoff position	x		yz		U (Å^2)		
Ba	2c	0	*0*	0	*0*	½	*½*	0.0018(7)
Co	4e	0	*0*	0.7100(4)	*0.7960*	0	*0*	0.001(1)
Mg1	8n	0.6992(2)	*0.6692*	0.8296(1)	*0.7986*	½	*½*	0.0084(4)
Mg2	2b	0	*0*	½	*½*	0	*0*	0.0246(8)
D1	8m	½	*½*	0.2931(1)	*0.2934*	0.2496(4)	*0.2393*	0.0544(5)
D2	8n	0.6891(2)	*0.6966*	0.8579(1)	*0.8577*	½	*½*	0.0544(5)
D3	4g	0.7932(4)	*0.7974*	0	*0*	0	*0*	0.0544(5)
Lattice parameter (Å)		7.392(2)	*7.2331*	11.602(4)	*11.5250*	4.6265(9)	*4.5641*	

Table 2. Selected distances (<3 Å) and angles for $BaD_2Mg_5[Co(-I)D_4]_2$, SU in parentheses. Experimental values are in normal type, those calculated by CASTEP are in italics.

Atoms	Distance(Å)	
Co-D1 x2	1.504(3)	*1.574*
D2 x2	1.605(3)	*1.590*
D2	2.520(2)	*2.544*
D2-D2	2.799(3)	*2.844*
D3	2.772(2)	*2.712*
D3	2.090(2)	*2.070*
Mg2-D2	2.159(2)	*2.171*
	Angle(deg)	
D1-Co-D1	100.59(9)	*98.25*
D1-Co-D2	108.238(2)	*107.02*
D2-Co-D2	121.33(9)	*126.86*

Table 3a. Metal atom positions and temperature parameters of $RbH_2Mg_5[Co(-I)H_4\ Ni(0)H_4]$, SU in parentheses

Atom	Wyckoff position	Occupancy	x	y	Z	U
Rb	2a	1	0	0	½	0.0109(7)
Co	4d	½	0	0.7032(1)	0.997(1)	0.0019(6)
Ni	4d	½	0	0.7032(1)	0.997(1)	0.0019(6)
Mg1	8e	1	0.7066(3)	0.8300(2)	0.996(3)	0.0267(9)
Mg2	2b	1	0	½	0.878(1)	0.022(2)

Table 3b . Metal atom positions and temperature parameters of $Rb_{0.41}Ba_{0.59}H_2Mg_5[CoH_4]_{1.59}[NiH_4]_{0.41}$, SU in parentheses

Atom	Wyckoff position	Occupancy	x	y	z	U Å
Rb	2a	0.41	0	0	½	0.008(1)
Ba	2a	0.59	0	0	½	0.008(1)
Co	4d	0.59	0	0.7054(3)	0.999(6)	0.0042(2)
Ni	4d	0.41	0	0.7054(3)	0.999(6)	0.000(1)
Mg1	8e	1	0.7021(9)	0.8309(5)	0.009(9)	0.015(3)
Mg2	2b	1	0	½	0.932(5)	0.015(7)
Lattice parameter (Å)			7.3811(2)	11.6594(3)	4.6445(1)	

Table 4. Lattice parameters, atom positions and temperature parameters of $SrD_2Mg_2[Co(I)D_5]$, SU in space group $P2_1/m$ (11), parentheses. Experimental values are in normal type, those calculated by CASTEP are in italics.

Atom	Wyckoff position	xy		z		U(Å^2)		
Sr	2e	0.7531(8)	*0.7510*	¼	*¼*	0.990(1)	*0.9985*	0.014(1)
Co	2e	0.758(2)	*0.7454*	¼	*¼*	0.499(4)	*0.4836*	0.038(3)
Mg1	2e	0.086(1)	*0.0803*	¼	*¼*	0.621(1)	*0.6240*	0.021(2)
Mg2	2e	0.425(1)	*0.4203*	¼	*¼*	0.373(1)	*0.3702*	0.006(1)
D1	2e	0.0760(6)	*0.0842*	¼	*¼*	0.9127(8)	*0.9227*	0.015(1)
D2	2e	0.5860(6)	*0.5756*	¼	*¼*	0.6398(7)	*0.6536*	0.023(1)
D3	2e	0.4194(7)	*0.4195*	¼	*¼*	0.0876(9)	*0.0733*	0.028(2)
D4	4f	0.6897(4)	*0.6901*	0.0162(9)	*0.4916*	0.3503(6)	*0.3496*	0.031(1)
D5	4f	0.1627(5)	*0.1611*	0.9946(9)	*0.9975*	0.3629(5)	*0.3465*	0.035(2)
Lattice parameter (Å)		7.818(2)	*7.725*	4.462(1)	*4.398*	6.640(2)	*6.467*	β=91.27(2)º *β=91.46º*

Table 5. Selected distances (<3Å) and angles for $SrD_2Mg_2[Co(I)D_5]$, SU in parentheses.

Atoms	Distance(Å)	
Co-D2	1.65(2)	*1.603*
D4 x2	1.52(2)	*1.566*
D5 x2	1.55(2)	*1.568*
D2-D4	2.345(6)	*2.422*
D5	2.204(5)	*2.252*
D5-D5	2.278(6)	*2.177*
D5	2.677(7)	*2.599*
D5	2.153(8)	*2.214*
D5	2.345(8)	*2.320*
	Angle(deg)	
D2-Co-D4	94.9(1)	*99.7*
D2-Co-D5	89.1(1)	*93.4*
D4-Co-D4	86.4(2)	*87.9*
D4-Co-D5	91.8(2)	*91.8*
D5-Co-D5	89.8(2)	*85.5*

Table 6. Lattice parameters, Space groups and lattice parameters for the investigated compounds

Compound	$BaH_2Mg_5[Co(-I)D_4]_2$	$RbH_2Mg_5[CoH_4][NiH_4]$	$SrH_2Mg_2[CoD_5]$
Space group, Z	*Immm*, 2	*Imm2*, 2	$P12_1/n1$, 2
a, Å	7.392(2)	7.345(6)	7.818(2)
b, Å	11.602(4)	11.877(8)	4.462(1)
c, Å	4.6265(9)	4.703(3)	6.640(2)
β, deg	-	-	91.27(2)
R_p, %	1.65	2.07	2.97
R_{wp}, %	2.23	3.12	3.78

Table 7 Lattice parameters, atom positions and temperature parameters of $Mg_2[Co(I)D_5]$, SU in space group *P4nmm* (129), SU in parentheses. Experimental values[20] are in normal type, those calculated by CASTEP are in italics.

Atom	Wyckoff position	xyz					
Co	2c	¼	*¼*	¼	*¼*	0.256(2)	*0.2589*
Mg1	2a	¾	*¾*	¼	*¼*	0	*0*
Mg2	2b	¾	*¾*	¼	*¼*	½	*½*
D1	2c	¼	*¼*	¼	*¼*	0.497(2)	*0.4974*
D2	8j	0.4879(4)	*0.4974*	0.4879	*0.4974*	0.2257(3)	*0.2313*
Lattice parameter (Å)		4.463(4)	*4.435*	4.463(4)	*4.435*	6.593(6)	*6.526*

Table 8 Selected distances (<3Å) and angles for $Mg_2[Co(I)D_5]$, SU in parentheses. Experimental values[20] are in normal type, those calculated by CASTEP are in italics.

Atoms	Distance(Å)	
D2	1.515(3)	*1.562*
D1-D2	2.337(9)	*2.354*
D2-D2	2.124(3)	*2.195*
Mg1-D2	2.170(2)	*2.177*
D2	2.402(2)	*2.352*
	Angle(deg)	
D1-Co-D2	97.6(1)	*96.6*
D2-Co-D2	89.1(1)	*89.2*

Table 9. Observed and calculated (at the Γ-point) transition energies with mode descriptions for $BaH_2Mg_5[Co(\text{-}I)H_4]_2$. The observed spectrum can be seen in figure 4

Observed / cm^{-1}	Calculated / cm^{-1}	Description
75		Ba translation
97	97	Ba translation + $[Co(\text{-}I)H_4]$ translation
116	145	Mg translation+ $[Co(\text{-}I)H_4]$ libration
146	148	Mg translation+ $[Co(\text{-}I)H_4]$ libration
168	177	Mg translation+ $[Co(\text{-}I)H_4]$ libration
191	21	Mg translation+ $[Co(\text{-}I)H_4]$ translation
218	233	$[Co(\text{-}I)H_4]$ translation
234	241	Mg translation+ $[Co(\text{-}I)H_4]$ translation
249	250	Mg translation
250	268	Mg translation+ $[Co(\text{-}I)H_4]$ translation
279	319	Mg translation
379	395	$[Co(\text{-}I)H_4]$ libration
401	406	$[Co(\text{-}I)H_4]$ libration
408	470	$[Co(\text{-}I)H_4]$ libration
472	526	H–Co–H bend (ν_3 T_2)[a]
554	578	H–Co–H bend (ν_3 T_2)
582	632	H–Co–H bend (ν_3 T_2)
644	644	H–Co–H bend (ν_2 E)
649	672	H–Co–H bend (ν_2 E)[a]
656	712	Interstitial hydride translation
725	733	Interstitial hydride translation
948	958	Interstitial hydride translation
1678	1690	Co–H stretch (ν_3 T_2)
1711	1718	Co–H stretch (ν_3 T_2)
1791	1798	Co–H stretch (ν_3 T_2)
1803	1821	Co–H stretch (ν_1 A_1)

[a] Symmetry classification are for the $[Co(\text{-}I)H_4]^{4-}$ ion in T_d symmetry.[21]

Table 10. Observed and calculated (at the Γ-point) transition energies with mode descriptions for $SrH_2Mg_2[Co(I)H_5]$. The observed spectrum can be seen in figure 4

Observed / cm^{-1}	Calculated / cm^{-1}	Description
92	Ba translation	
102	107	Ba translation
108	118	$[Co(I)H_5]$ translation
157	165	$[Co(I)H_5]$ translation
167	178	$[Co(I)H_5]$ translation
198	211	Mg translation
223	232	Mg translation
235	237	Mg translation
244	254	Mg translation
260	263	Mg translation
279	315	Mg translation
510	545	$[Co(I)H_5]$ libration
547	580	$[Co(I)H_5]$ libration
584	632	$[Co(I)H_5]$ libration
590	616	H–Co–H bend (ν_5 B_1)[a]
582	637	Interstitial hydride translation
670	683	Interstitial hydride translation
761	768	H–Co–H bend (ν_3 A_1)
757	778	Interstitial hydride translation
795	810	Interstitial hydride translation
863	867	H–Co–H bend (ν_8 E)
875	882	H–Co–H bend (ν_8 E)
889	893	H–Co–H bend (ν_9 E)
926	927	H–Co–H bend (ν_9 E)
999	1005	H–Co–H bend (ν_6 B_2)
1035	1042	Interstitial hydride translation
1058	1085	Interstitial hydride translation
1618	1623	Axial Co–H stretch (ν_1 A_1)

1703	1727	Equatorial Co–H stretch (ν_7 E)
1753	1754	Equatorial Co–H stretch (ν_7 E)
1805	1809	Equatorial Co–H stretch (ν_2 A_1)
1815	1818	Equatorial Co–H stretch (ν_4 B_1)

[a]Symmetry classification are for the $[Co(I)H_5]^{4-}$ ion in C_{4v} symmetry.[19,21]

Figures

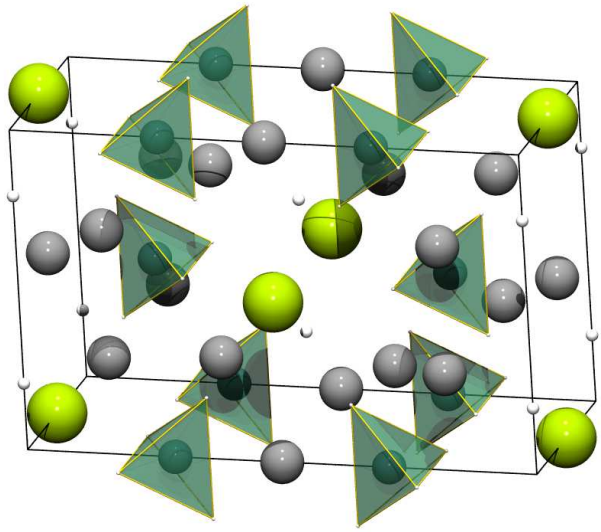

Figure 1. $BaD_2Mg_5[Co(\text{-}I)D_4]_2$ Z=2. $[Co(\text{-}I)D_4]$ are represented as green tetrahedra, Ba as lime green spheres and Mg as grey spheres

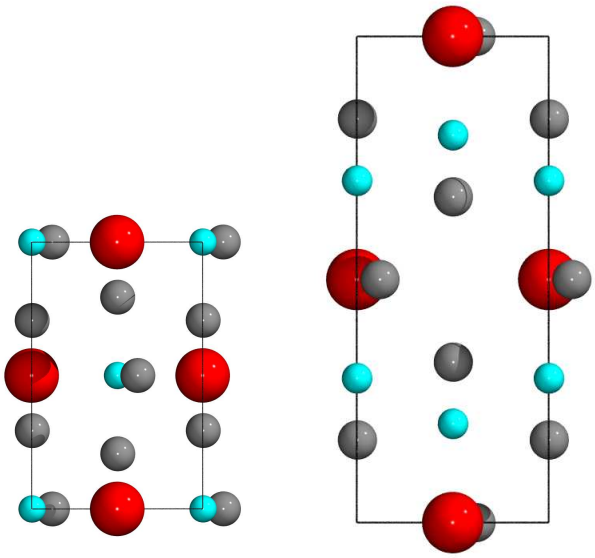

Figure 2. $RbH_2Mg_5[Co(\text{-}I)H_4$ $Ni(0)H_4]$ Projected in the [100] direction (left) and the [001] direction (right) showing how Mg2 has moved from the position 0.0, 0.5, 0 as Co is

exchanged for Ni and Ba is exchanged for Rb. This lowers the symmetry from to *Immm* (71) to *Imm2* (44). Red, cyan, grey spheres denote Rb, Co/Ni and Mg respectively

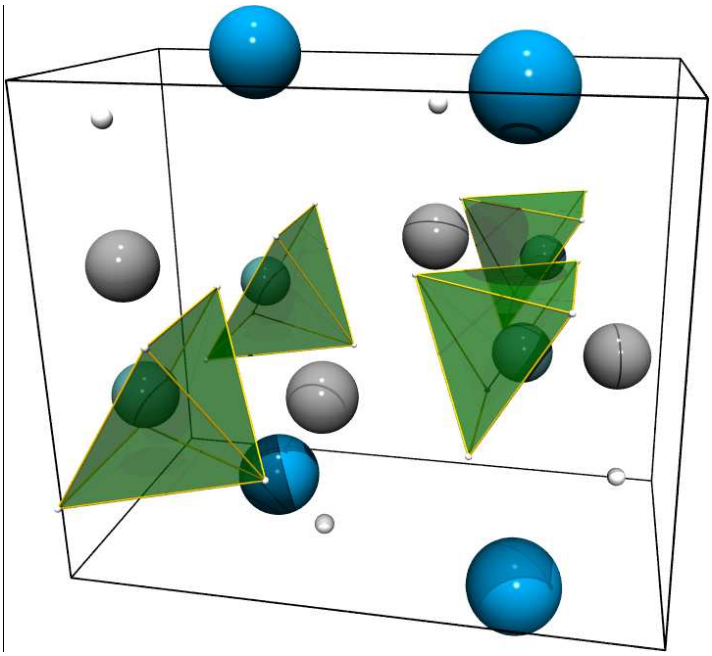

Figure 3. Structure of $SrD_2Mg_2[Co(II)D_5]$ Z=2. $[Co(II)D_5]$ are represented as green square pyramids, Sr as blue spheres and Mg as grey spheres

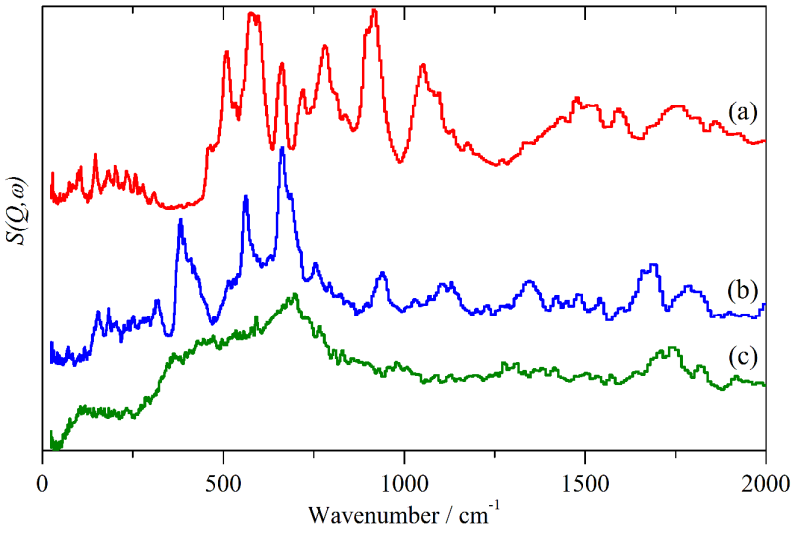

Figure 4. INS spectra recorded on TOSCA at 10 K of: (a) $SrH_2Mg_2[Co(I)H_5]$ (b) $BaH_2Mg_{10}[Co(-I)H_4]_2$ and (c) $RbH_2Mg_{10}[Co(-I)H_4\ Ni(0)H_4]$.

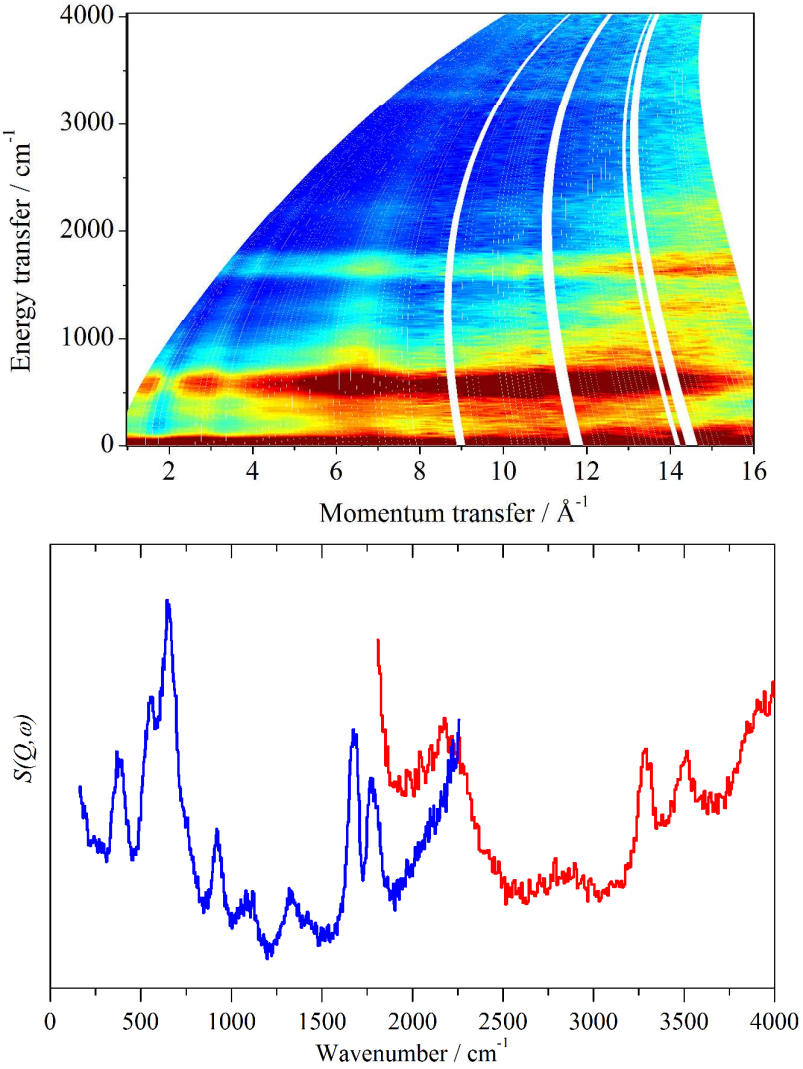

Figure 5. INS spectra recorded on MAPS at 10 K of $BaH_2Mg_{10}[Co(\text{-}I)H_4]_2$. Upper: $S(Q,\omega)$ map (E_i = 4033 cm^{-1}). Lower: MAPS spectra obtained by summing over momentum transfer for E_i = 2420 cm^{-1} (blue trace) and E_i = 4033 cm^{-1} (red trace). The red trace is ×4 ordinate expanded relative to the blue trace.

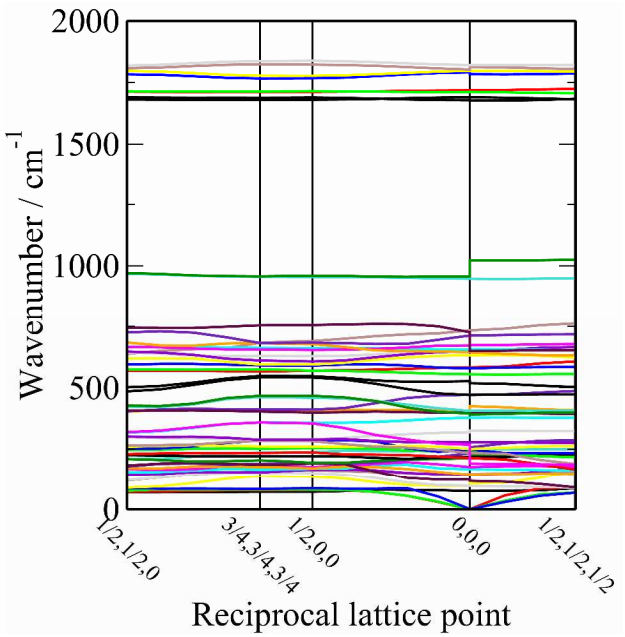

Figure 6. Dispersion curves for $BaH_2Mg_5[Co(-I)H_4]_2$.

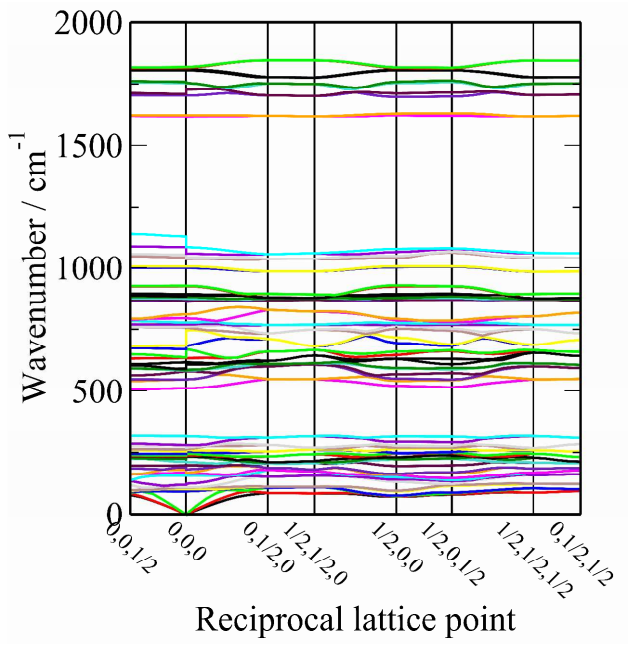

Figure 7. Dispersion curves for $SrH_2Mg_2[Co(I)H_5]$.

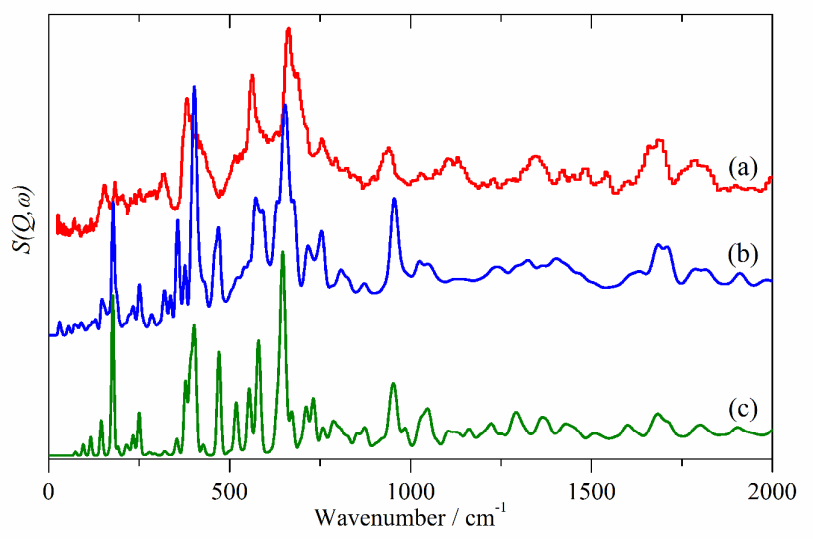

Figure 8. Comparison of INS spectra of $BaH_2Mg_5[Co(-I)H_4]_2$: (a) experimental, (b) generated from the calculation across the entire Brillouin zone and (c) generated from a Γ-point only calculation

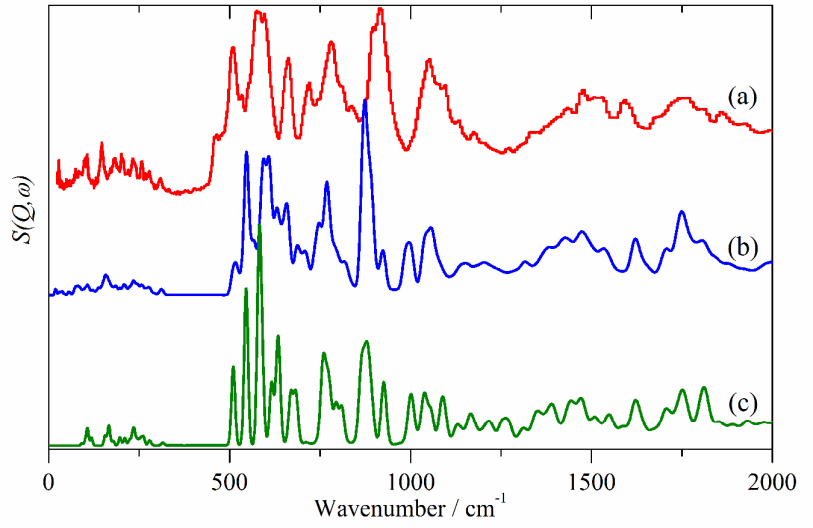

Figure 9. Comparison of INS spectra of $SrH_2Mg_2[Co(I)H_5]$: (a) experimental, (b) generated from the calculation across the Brillouin zone and (c) generated from a Γ-point only calculation

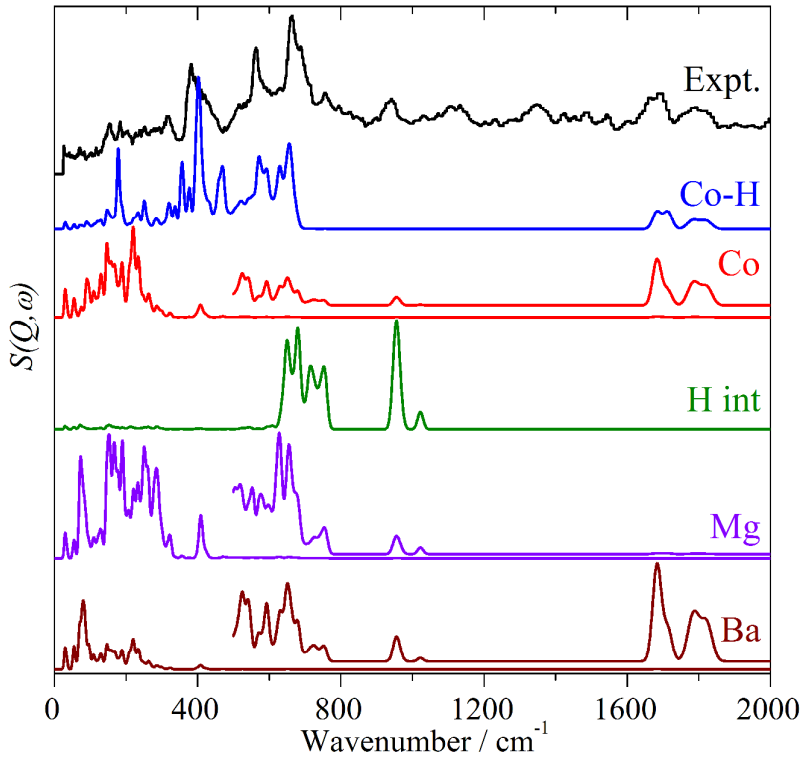

Figure 10. Comparison of the experimental (Expt., black) INS spectrum of $BaH_2Mg_5[Co(-I)H_4]_2$ with those generated by including only the motions of the hydrides bonded to the cobalt (Co–H, blue), the cobalt atoms (Co, red), the interstitial hydrides (H int, olive), the magnesium ions (Mg, violet), and the barium ions (Ba, brown). The insets in the spectra of Co, Mg and Ba are ordinate expansions of the region 500 – 2000 cm^{-1} with factors of 50, 80 and 300 respectively.

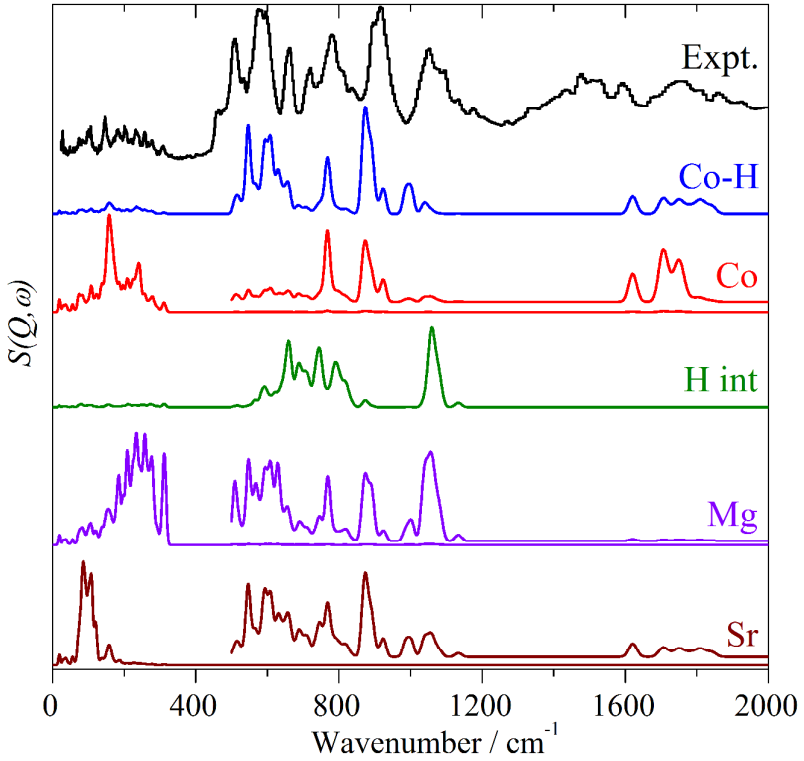

Figure 11. Comparison of the experimental (Expt., black) INS spectrum of $SrH_2Mg_2[Co(I)H_5]$ with those generated by including only the motions of the hydrides bonded to the cobalt (Co–H, blue), the cobalt atoms (Co, red), the interstitial hydrides (H int, olive), the magnesium ions (Mg, violet), and the strontium ions (Sr, brown), only the $0 \rightarrow 1$ transitions are shown. The insets in the spectra of Co, Mg and Ba are ordinate expansions of the region 500 – 2000 cm^{-1} with factors of 50, 100 and 400 respectively.

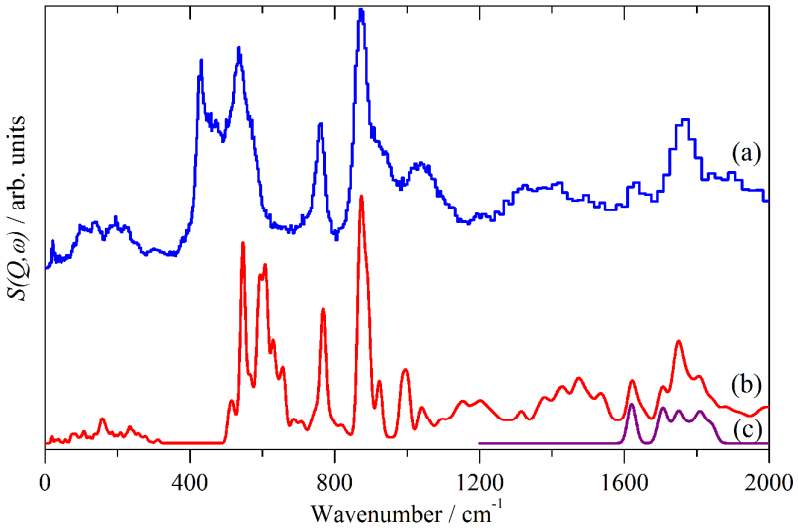

Figure 12. Comparison of the (a) experimental INS spectrum of $Mg_2[Co(I)H_5]$ and (b) that of the $[Co(I)H_5]^{4-}$ in $SrH_2Mg_2[Co(I)H_5]$ generated by considering only the hydrides bonded to the cobalt. To aid the comparison all transitions ($0 \rightarrow 1$, $2 \cdots 10$) are included, (c) as (b) but only the $0 \rightarrow 1$ transitions for the 1200 – 2000 cm^{-1} region are shown.

References

(1) Miller, G. J.; Deng, H.; Hoffmann, R. *Inorg. Chem.* **1994**, *33*, 1330–1339.

(2) Häussermann, U.; Blomqvist, H.; Noréus, D. *Inorg. Chem.* **2002**, *41*, 3684–3692.

(3) Lelis, M.; Milcius, D.; Wirth, E.; Hålenius, U.; Eriksson, L.; Jansson, K.; Kadir, K.; Ruan, J.; Sato, T.; Yokosawa, T. *J. Alloys Compd.* **2010**, *496*, 81–86.

(4) Kadir. K.; Noréus D.; Inorg. Chem. **2007**, 46, 2220 and Inorg. Chem. **2009**, 48, 3288

(5) Werner, P. E.; Eriksson, L.; Westdahl, M. *J. Appl. Crystallogr.* **1985**, *18*, 367–370.

(6) Favre-Nicolin, V.; Černý, R. *J. Appl. Crystallogr.* **2002**, *35*, 734–743.

(7) Larson, A. .; Dreele, R. B. Von *Los Alamos National Laboratory Report* **1994**, 86–748.

(8) Refson, K. *Phys. Rev. B* **2006**, *73*, 1–12.

(9) Clark, S. J.; Segall, M. D.; Pickard, C. J.; Hasnip, P. J.; Probert, M. I. J.; Refson, K.; Payne, M. C. *Zeitschrift für Kristallographie* **2005**, *220*, 567–570.

(10) Ceperley, D. M. *Phys. Rev. Lett.* **1980**, *45*, 566–569.

(11) Perdew, J. P., Zunger, A. *Phys. Rev. B* **1981**, *23*, 5048–5079.

(12) Rappe, A.; Rabe, K.; Kaxiras, E.; Joannopoulos, J. *Phys. Rev. B* **1990**, *41*, 1227–1230.

(13) Ramirez-Cuesta, a. J. *Comput. Phys. Commun.* **2004**, *157*, 226–238.

(14) P. C. H. Mitchell, S. F. Parker, A. J. Ramirez-Cuesta, J. T. *Vibrational spectroscopy with neutrons, with applications in chemistry, biology, materials science and catalysis*; World Scientific, 2005.

(15) Parker, S. F. *Coord. Chem. Rev.* **2010**, *254*, 215–234.

(16) www.isis.stfc.ac.uk.

(17) Perdew, J.; Burke, K.; Ernzerhof, M. *Phys. Rev. Lett.* **1996**, *77*, 3865–3868.

(18) Parker, S. F.; Refson, K.; Williams, K. P. J.; Braden, D. a; Hudson, B. S.; Yvon, K. *Inorg. Chem.* **2006**, *45*, 10951–7.

(19) Parker, S. F.; Jayasooriya, U. A.; Sprunt, J. C.; Bortz, M.; Yvon, K. *Journal of the Chemical Society, Faraday Transactions* **1998**, *94*, 2595–2599.

(20) Zolliker, P.; Yvon, K.; Fischer, P.; Schefer, J. *Inorg. Chem.* **1985**, *24*, 4177–4180.

(21) Nakamoto, K. *Infrared and Raman Spectra of Inorganic and Coordination Compounds, Part A: Theory and Applications in Inorganic Chemistry 5th ed.*; John Wiley and Sons, New York, 1997.

TOC picture